



# Brief communication: Vent opening at Campi Flegrei – clues from dyke propagation patterns

Jacopo Selva<sup>1,2</sup> and Nello Mangone<sup>1</sup>

<sup>1</sup>Dipartimento di Scienze della Terra, dell’Ambiente e delle Risorse (DiSTAR), University of Naples Federico II, Naples, Italy

<sup>2</sup>Istituto Nazionale di Geofisica e Vulcanologia, Osservatorio Vesuviano, Naples, Italy

**Correspondence:** Jacopo Selva (jacopo.selva@unina.it)

Received: 5 August 2025 – Discussion started: 18 August 2025

Revised: 16 April 2026 – Accepted: 23 April 2026 – Published: 3 June 2026

**Abstract.** Forecasting future vent opening position is fundamental for managing volcanic hazards, and is usually based on the spatial density of past vents or other crust weakness indicators. Here, a novel empirical approach inspired by dyke propagation models is applied to the Campi Flegrei caldera. Results show that dyke azimuthal direction and propagation length are statistically independent, that azimuth correlates with topographic peaks within 7 km from the caldera centre, and that propagation length exhibits two main peaks at 2 and 4 km. Based on these results, we develop two new vent opening probability maps with maxima well correlating with caldera’s structure and recent seismicity.

## 1 Introduction

The Campi Flegrei caldera volcanic activity dates back to the upper Pleistocene, with the earliest volcanic activity observed in outcrops estimated at approximately 80 kyr (Pappalardo et al., 1999; Scarpati et al., 2013). Recent studies identified widespread tephra layers originated from Campi Flegrei, extending its activity to nearly 200 kyr (e.g., Monaco et al., 2022; Fernandez et al., 2024; Sparice et al., 2024). The first caldera collapse occurred approximately 39 000 years ago with the Campanian Ignimbrite (CI) eruption (Giaccio et al., 2017). A second major eruption occurred around 14 000 years ago, the Neapolitan Yellow Tuff (NYT), possibly causing a second collapse, after which volcanic activity resumed within the caldera (Orsi et al., 2004).

The post-NYT eruptive history is divided into three main epochs (Di Vito et al., 1999; Bevilacqua et al., 2016; Fig. 1). The first epoch comprises at least 33 eruptions, spanning

from 14 000 to 10 600 years ago. The eruptive vents align with the caldera boundaries, with the most energetic eruption being that of the “Pomici Principali” around 12 000 years ago (Bevilacqua et al., 2016). The second epoch follows a relatively brief quiescent period and includes nine eruptions dated between 9600 and 9100 years ago, primarily concentrated in the northeastern sector of the caldera. The third epoch encompasses a total of 26 eruptions from approximately 5500 to 3800 years ago. Its activity was predominantly focused in the northeastern part of the caldera (Agnano area), secondarily in the northwestern sector (Averno area), and concluded with peripheral distal eruptions (Nisida, Capo Miseno, and Fossa Lupara, Natale et al., 2025). The most energetic eruption during this period was that of Agnano-Monte Spina around 4500 years ago (Bevilacqua et al., 2016). The long period of quiescence following the third epoch lasted until 1538 AD, when the Monte Nuovo eruption took place in the northwestern sector of the caldera (Di Vito et al., 2016). The caldera has not experienced any eruption since.

After NYT, the caldera experienced significant resurgence, accompanied by seismicity, degassing, and slow ground deformation often referred to as bradyseism (Isaia et al., 2019; Natale et al., 2022). The latter is centred mainly in the Pozzuoli area, which is approximately at the centre of the caldera (Fig. 1), and major movements were tracked at least from the 4th century AD thanks to the ruins of a Roman temple in the port of this city, the Serapeum (Di Vito et al., 2016; Vitale and Natale, 2023). The largest known bradyseismic events are the ones related to the last Campi Flegrei eruption (the 1538 Monte Nuovo eruption, Di Vito et al., 2016). In the last century, three main bradyseismic crises occurred in

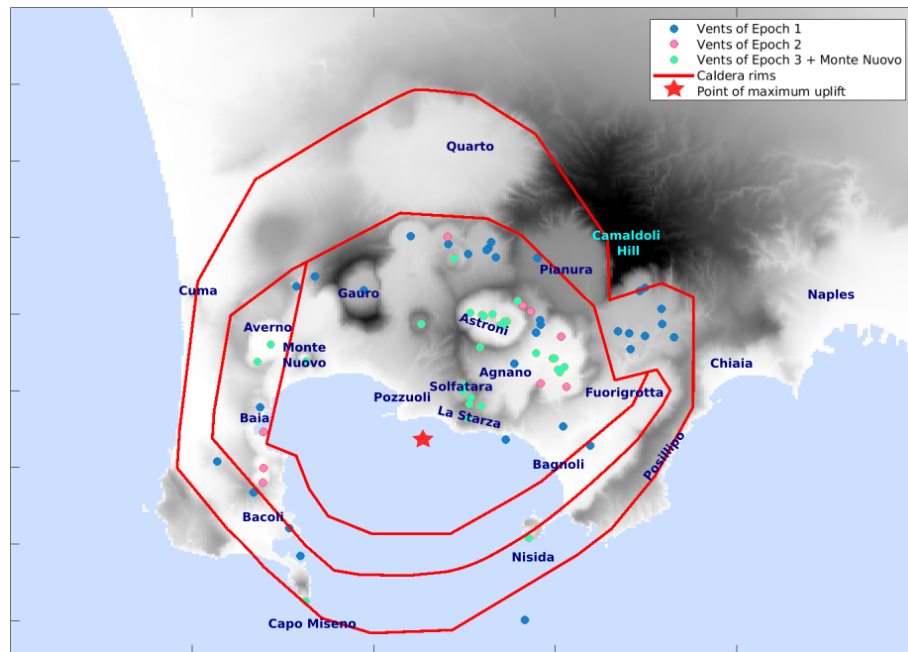


**Figure 1.** Topographic map of the Campi Flegrei caldera, along with the vent positions of post-NYT eruptions (from Bevilacqua et al., 2016) and the caldera rims active in the last 40 ka (Natale et al., 2024, 2025). For simplicity, Monte Nuovo is included in Epoch 3. Darker colours mean higher elevations.

1950–52, 1970–72, and 1982–84, characterised by episodes of uplift of almost 2 m interrupting a slow long-lasting subsidence (Del Gaudio et al., 2010). Approximately in 2005, a slow uplift started, accelerating over time, which fully recovered the subsidence in 2021, and now exceeds the uplift peaks observed in the last century (Bevilacqua et al., 2024). This event is still ongoing.

Forecasting vent opening is crucial for any volcanic hazard quantification. Different approaches were adopted at Campi Flegrei through time. Alberico et al. (2002) developed a method identifying crustal weaknesses using geophysical, geological, and geochemical parameters. Their probability map indicates the highest likelihood of vent openings in the central caldera near Pozzuoli (Fig. 1). Selva et al. (2012) utilized a Bayesian approach fed by fewer parameters, focusing on tectonic structures recognized at that time, to track crust weakness, and past vents, shifting the area at higher probability toward the northeastern and northwestern sectors, where post-NYT activity concentrated. Bevilacqua et al. (2015) adopted a method based on Gaussian kernel and accounting for the uncertainty on past vent positions, confirming the northeastern sector (near Agnano and Astroni, Fig. 1) as the most likely area for future eruptions. Both Selva et al. (2012) and Bevilacqua et al. (2015) included also a formal quantification of the epistemic uncertainty in their models, accounting for model uncertainty. More recently, based on past observations and removing multiple eruptions from clustered vents, Charlton et al. (2020) noted that vent opening occurred substantially randomly within a ring area sur-

rounding the caldera centre, corresponding to the caldera rim (Fig. 1), producing a new qualitative indication about potential future vent opening.

Rivalta et al. (2019) studied the physical propagation of magma dykes by modelling the trajectory of potential dykes due to the subsurface stress field and the dike's initial position. Their model accounts for various stresses affecting magma ascent. For calderas, it suggests that eruptive vents are concentrated at specific distances from the centre, influenced by the stress induced by the caldera depression, defining a higher propensity to eruption closer to caldera rims, as noted by Charlton et al. (2020). Considering the caldera depression size, Rivalta et al. (2019) forecasted for Campi Flegrei a potential peak for vent opening at a semi-annular belt located between 2.3 and 4.2 km from the caldera centre. Rivalta et al. (2019) analysed also the effect of caldera unloading, as well as those of topographic peaks, which may break the caldera symmetry. They analysed the case of the Campi Flegrei caldera, explaining the concentration of volcanic activity in the northeastern sector due to the topographic peak of the Camaldoli Hill (Fig. 1), which creates a stress field that may favour magma trajectories in the north-east direction.

The main features of Rivalta et al. (2019) model are (i) that the geometry of the caldera (unloading effect) significantly influences dykes propagation outward, promoting eruptions away from the geometric centre of the caldera, and (ii) topographic asymmetries create localised stress variations in the subsurface, affecting eruption frequency across different angular sectors. While a sufficiently detailed knowledge of the

sub-surface stress state is difficult to reach, it is possible to verify if these two main features left a trace on the available record of past vent positions, and to use this empirical signature to define new vent opening probability maps.

## 2 Method

Rivalta et al. (2019) found that the path of the dykes feeding eruptions is mainly controlled by the geometry of the caldera, which determines the distance from the centre of the caldera, and by the topographic peaks surrounding the caldera, which establishes preferential directions for propagation. To this end, for Campi Flegrei Rivalta et al. (2019) assumed that the origin at depth of the magma is an oblate volume located at the centre of the caldera, 3 km below the location of the maximum observed uplift (Amoruso et al., 2014a; Rivalta et al., 2019; Buono et al., 2025), and producing mostly lateral propagation with trajectories controlled by the structure of the caldera and the consequent stress distribution within the caldera. In other words, Rivalta et al. (2019) demonstrate that, in an approximately symmetric caldera with a given magma source located around the centre of the caldera, independently of its specific depth and size, we expect a symmetrical radial dyke propagation from the source, and with preferred directions controlled by local factors. The empirical track of these features may be retrieved by studying the distribution of past vents around the caldera centre, being this position not necessarily the origin point for dykes, which may indeed detach from the edge of the source (Gregg et al., 2012; Rivalta et al., 2019), but simply the reference for tracking the radial symmetry.

Assuming a similar magma origin also for future eruptions, these empirical distributions can then be used to set a vent opening probability map. The probability density function in a specific point in the caldera can be calculated in polar coordinates using the following formula:

$$f_{\text{pol}}(r, \theta) = f_r(r) f_{\theta}(\theta), \quad (1)$$

where the term  $f_r(r)$  is the probability distribution for the distances from the centre of the caldera, and the term  $f_{\theta}(\theta)$  is the angular probability distribution. In this formulation, it is assumed that these two distributions can be considered independent. Indeed, the physical process described in Rivalta et al. (2019) suggests a potential independence between direction of dyke propagation and distance from the caldera centre, as they are controlled by two different features of the caldera, being the distance fundamentally controlled by the size of the nearly circular shape of the caldera, and the direction predominantly controlled by local topographic features. This independence should also leave an empirical track in past vent positions, which can also be formally verified by testing whether the direction and the distances found using past vent positions are correlated to each other.

The probability distribution of Eq. (1) can be transformed into Cartesian coordinates as follows:

$$f_{xy}(x, y) = \frac{1}{r} f_{\text{pol}}(r, \theta) = \frac{1}{r} f_r(r) f_{\theta}(\theta), \quad (2)$$

where the term  $f_{\text{pol}}(r, \theta)$  is again factorized in its two terms using Eq. (1). Defining an application grid, Eq. (2) can be used to establish a vent probability map by substituting  $f_r(r)$  and  $f_{\theta}(\theta)$  with the appropriate distributions of potential distance-from-centre and azimuth. Depending on the available data, such distributions may be estimated empirically, looking at the distribution of past vents, including all the data that reflect the present state of the caldera, or analysing the topographical peaks surrounding the caldera.

## 3 Results

At Campi Flegrei, an oblate central pressurized melt zone located at the center of the caldera is compatible with many geophysical evidences (e.g. Barberi et al., 1991; Capuano et al., 2013; Castaldo et al., 2021; De Landro et al., 2025). Inflation of a caldera-centered oblate spheroidal magma chamber at a depth of  $\sim 3.5$  km is consistent with the deformation in the last  $\sim 600$  years at least (Di Vito et al., 2016; D'Auria et al., 2015; Amoruso et al., 2007, 2014b), and a similar source is likely active at least in the last 5 ka (Di Vito et al., 2016; Rivalta et al., 2019). The position of the caldera centre is here assumed at the point of maximum uplift, here set 800 m south of the GNSS station of Rite at coordinates Easting 426355 and Northing 4518743 (UTM WGS84, zone 33N; Bevilacqua et al., 2024, Fig. 1). To establish an empirical model, we study the empirical distribution of azimuth (angle to the North of the line connecting the centre of the caldera and the vent, hereinafter azimuth) and of the distance from the centre of the caldera (hereinafter distance) of past eruptions. We consider the 71 vent positions of the post-NYT activity (Bevilacqua et al., 2016). The stability of these empirical distributions on the specific location of the caldera center is tested by sampling other possible centers in boxes of 1 and 2 km around the selected centre (Fig. S1 in the Supplement). Past vent positions are also affected by significant uncertainty. To evaluate its potential impact on all statistical analyses, we consider the uncertainty bounds defined in Bevilacqua et al. (2016), accounting for the uncertainty by randomly sampling 1000 alternative synthetic positions uniformly distributed within the defined uncertainty bounds (Fig. S1).

### 3.1 Empirical distributions of distance and azimuth

We first analyse the distances between the centre of the caldera and all post-NYT vents. The analysis is conducted separately for the three epochs. For simplicity, the recent Monte Nuovo eruption is included in the third epoch. In Fig. 2A, we report the empirical distributions (histograms with bins of 250 m, the corresponding empirical cumulative

distributions are reported in Fig. S2), revealing a strong difference between the first epoch, where 60 % of eruptions occur between 4400 and 6600 m, and the third epoch that shows shorter distances, with two significant peaks around 4000 and 2000 m, being Epoch 2 somehow intermediate between the other two. The results are stable for different selected centers of the caldera (Fig. S3).

To test if the distributions for the different Epochs are different, we implement a two-sample Kolmogorov–Smirnov test (KS2), a non-parametric statistical test used to determine if two independent datasets are drawn from the same underlying distribution (Gibbons and Chakraborti, 2003). Here and in the following tests, the significance level (red line in figures) is set to 0.01 and it is corrected for multiple testing using the Bonferroni (1936) criterion, which consists of dividing the significance level by the number of comparisons. The test confirms that the difference between Epoch 1 and Epoch 3 is statistically significant also accounting for vent position uncertainty (see Fig. S4), confirming the already observed progressive inward migration of post-NYT volcanism (Rivalta et al., 2019).

Following Rivalta et al. (2019), the direction of propagation of the dykes is controlled by topographic asymmetries. This direction can be investigated by analysing the azimuth of past vents with respect to the centre of the caldera. In Fig. 2B, we report the empirical distributions for the different epochs (histogram with bins of 20°, the corresponding empirical cumulative distribution functions are reported in Fig. S2), showing that most of eruptions have an azimuth toward NE (50°, toward Astroni, Agnano, and Solfatara). Also in this case, the results are stable for different selected centers of the caldera (Fig. S3). No specific differences between the distributions are visible. This observation is tested again with a two-sample Kolmogorov–Smirnov test (see Fig. S4), confirming that the directions of dyke propagation are similar in all epochs.

Rivalta et al. (2019) suggest that preferential directions may be induced by topographic peaks that locally modify the stress field, which is mainly controlled by unloading. To investigate this empirically, we analyse the maxima of the topography surrounding the caldera, retrieving the maxima in all directions in swaths with different length, hereinafter called radius. Maximum radii from 1 to 9 km are tested: for each radius, the profile of topographic maxima as a function of azimuth is normalised and compared with the azimuthal distribution of past eruptions (Fig. 2C). For simplicity, the present day topography is adopted, even if some of the edifices (and the corresponding topographic peaks) were built throughout the post-NYT activity. The comparison confirms the correlation anticipated by Rivalta et al. (2019). The primary peak is NE (around 50°) corresponds to the topographic peak associated with Accademia and La Pietra area (Fig. 1, for a radius of 1 km) and Camaldoli Hill (for radii of 3 km and larger). In agreement with Rivalta et al. (2019), the latter topographic peak is the most pronounced and it coincides

with the highest concentration of eruptive vents during various eruptive periods. A secondary peak appears in the NNW direction (around 330°) for intermediate radii (between 3 and 5 km), corresponding to the peak of the Gauro volcanic edifice (Monte Barbaro): this edifice was created during one of the first eruptions of the first epoch, and does not correspond to any peak in the observed distribution of azimuth. However, this secondary peak becomes less important for large radii (7 km and above), due to the prevalence of the Camaldoli Hill. Performing a Kolmogorov–Smirnov test between the angular distributions of past vents and of topographic peaks, the largest  $p$  values correspond to a maximum distance of 7 km. The null hypothesis of equal distribution is consistently not rejected independently from vent position uncertainty only for radii of 7 and 9 km, while it is rejected for smaller radii (Fig. S5).

### 3.2 Vent opening probability for Campi Flegrei

To apply Eq. (2) and quantify the vent probability map, we first test the independence of the radial and the azimuth distributions, by testing whether the direction and the distances of past vent positions are correlated to each other. To this end, we divide the directions in the 4 sectors (SW, NW, NE, and SE), and we compare the distribution of distances in the different sectors again using the Kolmogorov–Smirnov test. All the six couples are tested. The results (see Fig. S6) show that the hypothesis of equal distribution cannot be rejected for all combinations of sectors. This means that the distribution of distances in the different directions (with different azimuth) are statistically equal, standing for the independence between distance and azimuth.

To develop the probability map, we define a grid  $14.5 \times 12.5$  km, centred at Easting 427406 and Northing 4518958 (UTM WGS 84 33N), with 700 square cells  $500 \times 500$  m, equal to the one adopted in Selva et al. (2012). Then, the probability in each cell is computed by numerically integrating  $f_{xy}(x, y)$  computed through Eq. (2), where the terms  $f_r(r)$  and  $f_\theta(\theta)$  can be set using the empirical distributions developed in Sect. 3.1.

In particular, we propose 2 alternative implementations. At first, we consider for both  $f_r(r)$  and  $f_\theta(\theta)$  the empirical distributions that may be considered representatives of the present state of the caldera. Hereinafter, this first approach is referred to as model M1. To generalize the empirical distributions, we apply Gaussian kernels (red curves in Fig. 2A, C). The most appropriate bandwidth is defined using a leave-one-out technique with a Kullback–Leiber score (Connor et al., 2019). We set  $f_r(r)$  as the radial distribution of the eruptions of Epoch 3 only (including also Monte Nuovo), i.e. the most recent. As Epoch 1 is significantly different for the distribution of distances, its consideration would introduce a bias for forecasting future behaviours. Here, being very close in time to Epoch 1, Epoch 2 is assimilated to it, and only Epoch 3 is considered. The distribution is also

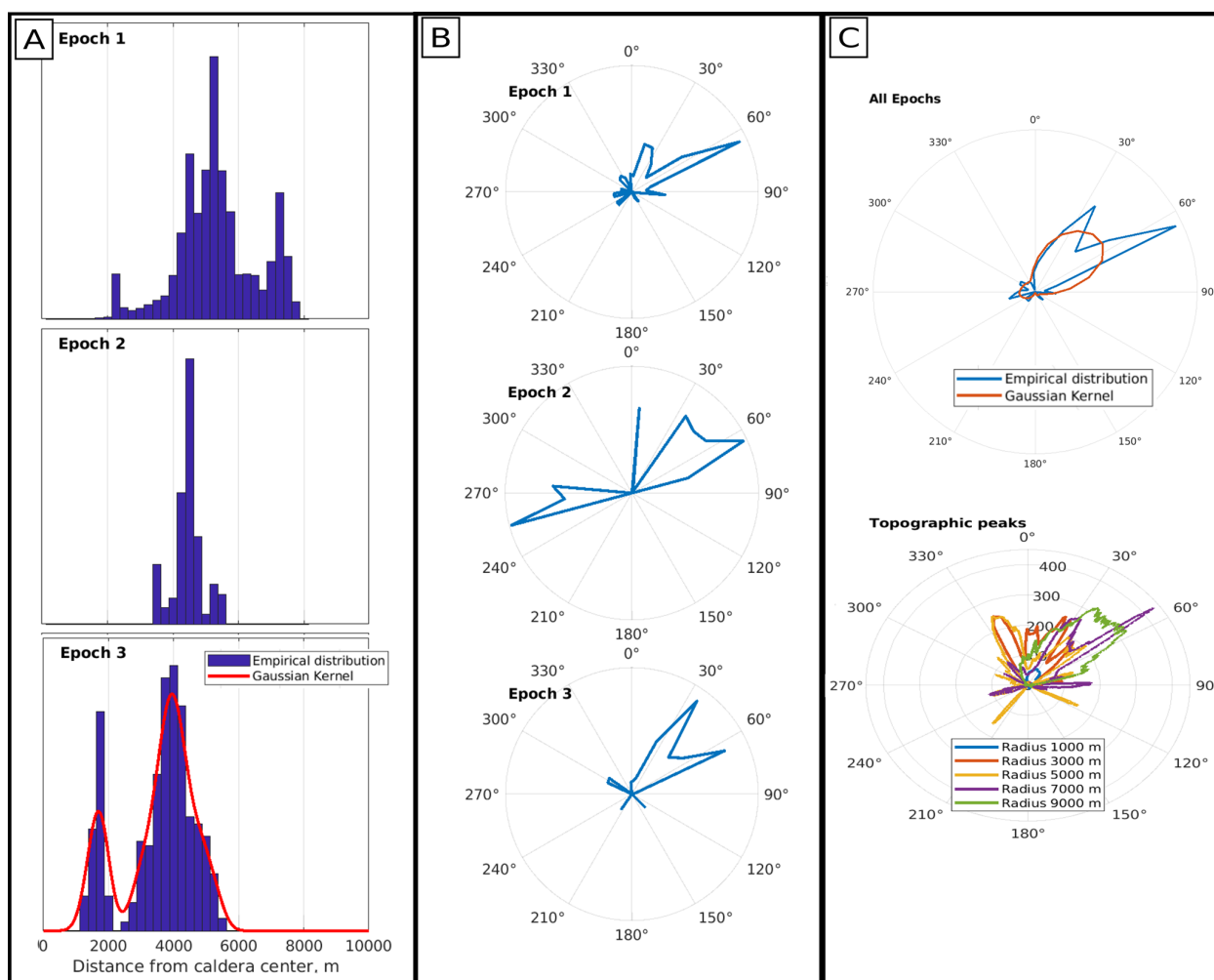


**Figure 2.** (A) Empirical distribution of distances from the centre of the caldera (dyke propagation length) for Epochs 1, 2 and 3. The red line in Epoch 3 reports a Gaussian kernel smoothing the empirical distribution. (B) Empirical distribution of azimuth (dyke direction) for Epochs 1, 2 and 3. (C) Empirical distribution of azimuth (dyke direction) for all Epochs (the red line in Epoch 3 reports a Gaussian kernel smoothing the empirical distribution) and the maxima of topographic peaks in radial swaths of variable length from the caldera centre.

truncated at 10 km, where it essentially drops to 0 (red line in Fig. 1A). The more appropriate bandwidth is found to be 275 m (Fig. S7a). To set  $f_{\theta}(\theta)$ , we instead consider the azimuth distribution of all post-NYT eruptions (red line in Fig. 1C), as the different epochs are statistically indistinguishable. For the kernel, the more appropriate bandwidth is found to be  $17^{\circ}$  (Fig. S7b).

A second implementation is also tested by setting  $f_{\theta}(\theta)$  differently, that is by substituting the empirical azimuth distribution adopted in M1 with the distribution of the topographic maxima for a radius of 7000 m, the one that better correlates with past vents. Hereinafter, this second approach is referred to as model M2.

The results of the two alternative implementations M1 and M2 are reported in Fig. 3. The numerical values for both models are reported as the Supplement. The resulting maps are similar, with two distinct probability peaks in the NE di-

rection at about 4 and 2 km from the centre, corresponding to the Agnano-Astroni and the Solfatara area, respectively. In M2, which considers the topographic contribution (Fig. 3B), the angular probability values are less smoothed than in model M1, where the empirical distributions are smoothed by the kernels (Fig. 3A). The effect is that the maximum probability values in the area at NE is almost halved in M1; also the relative peaks in the other directions appear relatively more evident in M2, with secondary peaks in the submerged side of the caldera toward W, in the direction of Bacoli, as well as the inland area toward NNW. On the contrary, in M1 probabilities are more distributed, generating two concentric and separated rings of larger probabilities at 2 and 4 km from the caldera centre.

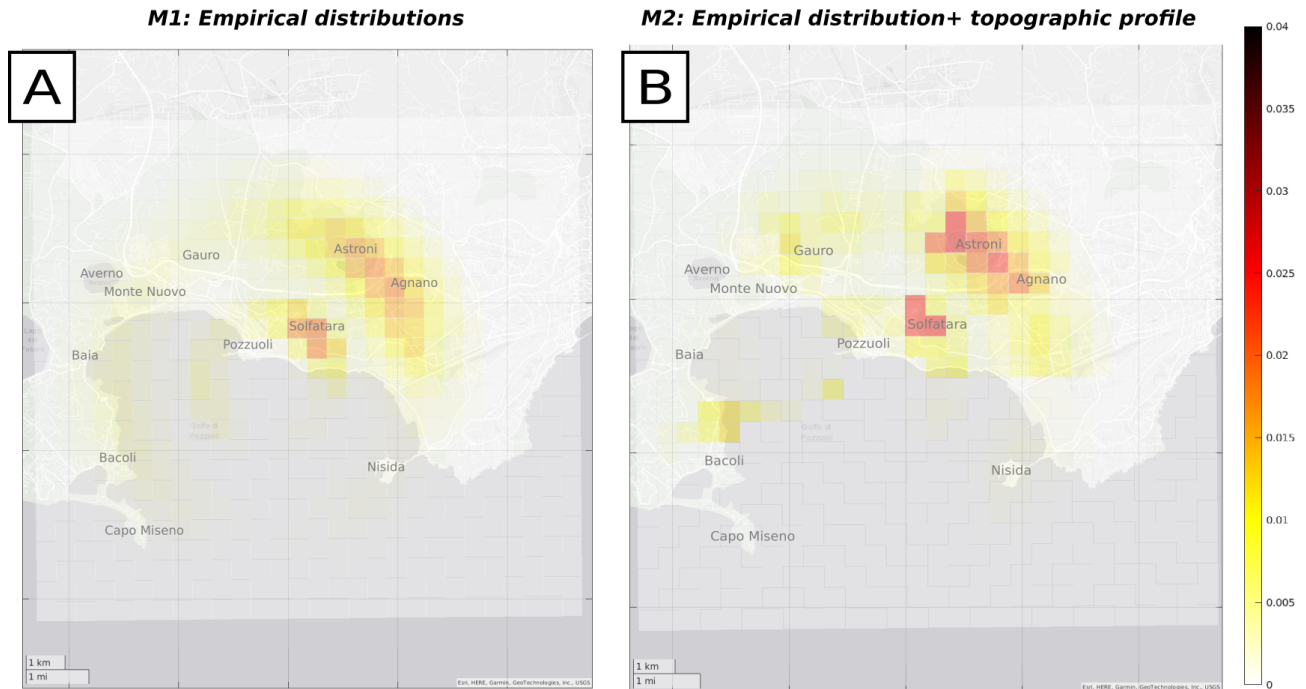


**Figure 3.** Vent opening probability maps: (A) model M1, based empirical distances and azimuth, (B) model M2, based on empirical distances and topographic azimuth (maps produced in Matlab, with data Esri, HERE, Garmin, GeoTechnologies, Inc., USGS|Powered by Esri).

#### 4 Discussion

Comparing these results with the main probability maps for Campi Flegrei discussed in the literature – Alberico et al. (2002), Selva et al. (2012), and Bevilacqua et al. (2015), hereinafter indicated as A02, S12 and B15, respectively – interesting coincidences and some significant differences emerge. As already noted, the map produced by A02 differs widely from S12 and B15 maps, having maximum values in the centre of the caldera, which is in contrast with the empirical evidence of recent past vents. In this, M1 and M2 are closer to S12 and B15, providing lower probabilities close to the caldera centre and larger probabilities in the NE area of Astroni and Agnano, where most of past vents concentrate.

To better highlight further similarities and differences, in Fig. 4A–F we report the maps of the relative differences in probability between M1, M2 and A02, S12, and B15, rescaling all of them to the same grid and, for S12 and B15, considering the mean of the epistemic uncertainty (Fig. S8). These maps highlight that the main differences are connected to the two ring regions with relatively higher probability discussed above, which were not present in previous studies.

The outer ring of relatively high probability, at 4 km, which coincides with the area identified by Charlton et al. (2020), includes the highest probability area of S12 and B15, located in the Agnano area to the NE of the caldera. However, also in this area, both M1 and M2 provide larger probabilities (Fig. 4, panels B, C, E, F). This ring also includes the area of Monte Nuovo (toward N, last eruption at

Campi Flegrei), and especially M1 provides larger probabilities than previous studies. Also the secondary peak identified in the Averno area (toward NW) in S12 is found in both M1 and M2, but shifted inward and eastward, in the direction of Gauro. The outer ring also generates several other secondary probability peaks at sea in the W direction, in the direction of the topographic peaks of Baia/Bacoli, especially in M1. These peaks are larger than in literature maps. On the other hand, in the areas of Nisida (toward SE) and Capo Miseno (toward SW), the probability values obtained here are relatively lower than the ones in the maps published in literature.

The inner ring of relatively high probability includes the high probability area of Solfatara, present in both S12 and B15, but also in this case both M1 and M2 provide larger probabilities (Fig. 4B, C, E, F). In addition, the inner ring introduces new peaks in probability within the bay, toward W, and in the coastal area of Accademia and La Pietra, toward E, both less pronounced in previous studies.

Also in the outer area of the caldera, external to the outer ring of relatively high probability, M1 and M2 are different than previous studies. Here, M1 and M2 do not assume that vent opening may occur only inside the caldera border, as in S12 and B15, but an outer limit is established only by the maximum observed distance from the centre of the caldera in Epoch 3, which is used to truncated the empirical distribution (Sect. 3.1). This cuts out the most external areas, mainly toward E, NW and S, where both M1 and M2 foreseen smaller probabilities than previous models.

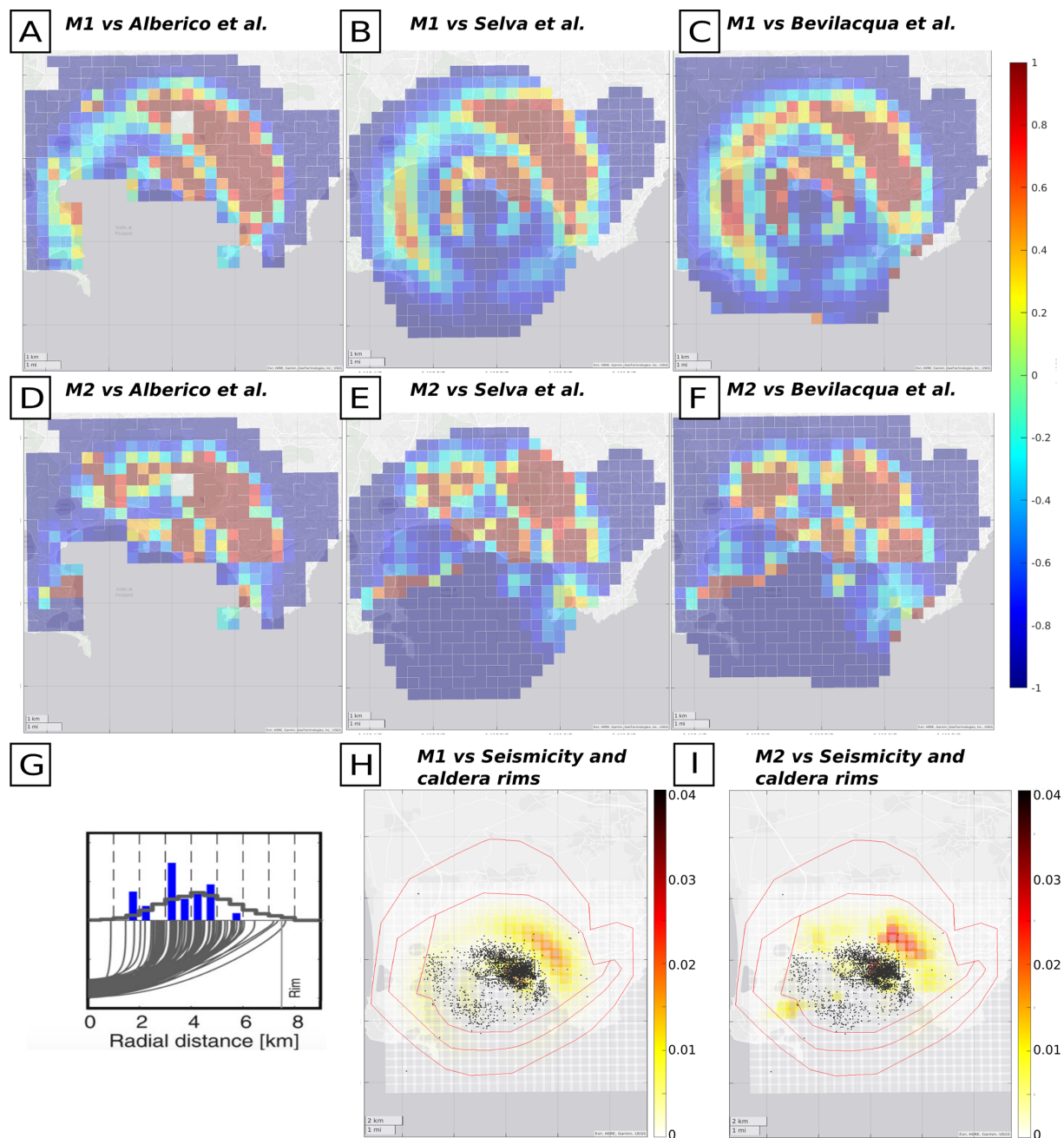


**Figure 4.** Relative difference between (A) M1 and Alberico et al. (2002), (B) M2 and Alberico et al. (2002), (C) M1 and Selva et al. (2012), (D) M2 and Selva et al. (2012), (E) M1 and Bevilacqua et al. (2015), (F) M2 and Bevilacqua et al. (2015). Relative differences are computed as the difference between our model (M1 or M2) and the literature model, divided by the literature model. Positive/negative numbers mean that M1/M2 are larger/smaller than literature studies, and a value equal to 1 means 100 % over-estimation (double) or larger. (G) Forecasted distances from the centre of the caldera from Rivalta et al. (2019) for dyke propagation compared with observed vent radii (blue bars). (H–I) Comparison between the spatial distribution of Campi Flegrei seismicity ( $M_d > 0.5$ ) in the period June 2023–June 2025, the caldera rims (as mapped in Natale et al., 2024, 2025), and M1 (H) and M2 (I). Maps produced in Matlab, with data Esri, HERE, Garmin, GeoTechnologies, Inc., USGS|Powered by Esri.

## 5 Conclusions

The vent opening maps derived in the study are based on assumptions radically different from the ones in literature. The approach is inspired from the dyke propagation model proposed in Rivalta et al. (2019), which suggests a substantial independence between the radial and azimuthal distributions of dykes propagating from a finite source located at the centre of the caldera. The results confirm some of the features already highlighted in previous studies, but also it introduces important differences. In particular, the most striking difference is that the vent probability peaks in two circles at around 2 and 4 km from the caldera centre, with significant modulations in the different directions, while smaller probabilities are found in the peripheral areas of the caldera. These rings of relatively higher probability, particularly evident in model M1 but present also in model M2, are compatible with in the range forecasted by Rivalta et al. (2019) when adopting only Epoch 3 data (Fig. 4G). However, the propagation distance distribution here produces two distinct peaks at 2 and 4 km, more than a continuous distribution in this range. The inner circle essentially coincides with an area characterized by high seismic activity recorded in the ongoing unrest episode (black dots in Fig. 4H, I), while the outer circle is instead closer to the position of the ring faults surrounding the inner caldera (red lines in Fig. 4H–I, Natale et al., 2024, 2025). These observations are completely independent and seem to spot privileged paths for magma ascent around the inner caldera border. This may be the subject of future studies.

It is important to stress that M1 and M2 are produced using the empirical distributions which are considered relevant for forecasting future occurrences, that is Epoch 3 for distances, and either all epochs or topographic peaks for azimuth. Indeed, while the distribution of the azimuth does not change significantly across epochs, the analysis of the distances with respect to the centre of the caldera has shown that Epoch 1 differs significantly from Epoch 3 in terms of distances. This may be sign of a change in the volcanic source and/or in the active stress field, in agreement with the findings of Rivalta et al. (2019), and with Orsi et al. (2004), who concluded that the last change in stress regime occurred prior to onset of the Epoch 3, and suggested that only the past 5 ka should be considered as reference for the present state of the caldera (Orsi et al., 2009). This assumption was adopted also in Selva et al. (2012).

Regarding the azimuth distribution, we found that the correlation between azimuth and topographic peaks is instead stable across epochs and is maximized considering the topographic peaks within 7 km from the caldera centre, demonstrating that the topography surrounding the caldera may be a good proxy for vent forecasting. In the future, this relationship may be better explored at different scales in space and time, studying for example the potential effects of the varying

spatio-temporal morphology due to eruption history, or the impact of different positions of the magma source.

Finally, even if we develop two maps, we prefer not to quantify the epistemic uncertainty on the proposed approach, differently from what was done in previous studies like Selva et al. (2012) and Bevilacqua et al. (2015). The reason is that several case studies recently demonstrated that the effective epistemic uncertainty on a target physical process (here vent opening) is better estimated by combining radically alternative approaches (e.g., defining weighted ensembles of alternative models), rather than by exploring the epistemic uncertainty inherent to one specific approach (Selva et al., 2018; Marzocchi et al., 2021; Meletti et al., 2021, among the others). Consequently, while the epistemic uncertainty on a given approach may be of relative interest, the very development of an alternative approach like the one presented here may be a significant added value to future quantification of epistemic uncertainty in the process of vent opening at Campi Flegrei, via multi-model ensembles or equivalent approaches that combine all the scientifically grounded approaches available in literature (e.g. SSHAC, 1997; Marzocchi et al., 2015, 2021).

*Code and data availability.* The numerical values for the probability maps M1 and M2 are reported as Supplement. The position of the vents related to past eruptions was obtained from Bevilacqua et al. (2015). The DEM used to find topographic peaks around Campi Flegrei is TINITALY (Tarquini et al., 2023) with WGS 84/UTM zone 33N coordinates, available at <https://doi.org/10.13127/tinality/1.1>.

*Supplement.* The supplement related to this article is available online at <https://doi.org/10.5194/nhess-26-2551-2026-supplement>.

*Author contributions.* JS and NM conceived and developed the Methodology. JS supervised the project. NM implemented the preliminary software for the analyses, with the support of JS. JS finalized the software and prepared the original draft. All the authors reviewed and approved the manuscript.

*Competing interests.* The contact author has declared that neither of the authors has any competing interests.

*Disclaimer.* Publisher's note: Copernicus Publications remains neutral with regard to jurisdictional claims made in the text, published maps, institutional affiliations, or any other geographical representation in this paper. The authors bear the ultimate responsibility for providing appropriate place names. Views expressed in the text are those of the authors and do not necessarily reflect the views of the publisher.

*Acknowledgements.* The figures and maps have been produced using Matlab and/or InkScape software. We thank the reviewers for the very constructive comments that allowed us to significantly improve the manuscript.

*Review statement.* This paper was edited by Giovanni Macedonio and reviewed by Craig Miller and two anonymous referees.

## References

- Alberico, I., Lirer, L., Petrosino, P., and Scandone, R.: A methodology for the evaluation of long-term volcanic risk from pyroclastic flows in Campi Flegrei (Italy), *J. Volcanol. Geoth. Res.*, 116, 63–78, [https://doi.org/10.1016/S0377-0273\(02\)00211-1](https://doi.org/10.1016/S0377-0273(02)00211-1), 2002.
- Amoruso, A., Crescentini, L., Linde, A. T., Sacks, I. S., Scarpa, R., and Romano, P.: A horizontal crack in a layered structure satisfies deformation for the 2004–2006 uplift of Campi Flegrei, *Geophys. Res. Lett.*, 34, L22313, <https://doi.org/10.1029/2007GL031644>, 2007.
- Amoruso, A., Crescentini, L., Sabetta, I., De Martino, P., Obrizzo, F., and Tammaro, U.: Clues to the cause of the 2011–2013 Campi Flegrei caldera unrest, Italy, from continuous GPS data, *Geophys. Res. Lett.*, 41, 1–7, <https://doi.org/10.1002/2014GL059539>, 2014a.
- Amoruso, A., Crescentini, L., and Sabetta, I.: Paired deformation sources of the Campi Flegrei caldera (Italy) required by recent (1980–2010) deformation history, *J. Geophys. Res.-Sol. Ea.*, 119, 858–879, <https://doi.org/10.1002/2013JB010392>, 2014b.
- Barberi, F., Cassano, E., La Torre, P., and Sbrana, A.: Structural evolution of Campi Flegrei caldera in light of volcanological and geophysical data, *J. Volcanol. Geoth. Res.*, 48, 33–49, [https://doi.org/10.1016/0377-0273\(91\)90031-T](https://doi.org/10.1016/0377-0273(91)90031-T), 1991.
- Bevilacqua, A., Isaia, R., Neri, A., Vitale, S., Aspinali, W. P., Bisson, M., Flandoli, F., Baxter, P. J., Bertagnini, A., Ongaro, T. E., Iannuzzi, E., Pistolesi, M., and Rosi, M.: Quantifying volcanic hazard at Campi Flegrei caldera (Italy) with uncertainty assessment: 1. Vent opening maps, *J. Geophys. Res.-Sol. Ea.*, 120, 2309–2329, <https://doi.org/10.1002/2014JB011775>, 2015.
- Bevilacqua, A., Flandoli, F., Neri, A., Isaia, R., and Vitale, S.: Temporal models for the episodic volcanism of Campi Flegrei caldera (Italy) with uncertainty quantification, *J. Geophys. Res.-Sol. Ea.*, 121, 7821–7845, <https://doi.org/10.1002/2016JB013171>, 2016.
- Bevilacqua, A., Neri, A., De Martino, P., Isaia, R., and Vitale, S.: Accelerating upper crustal deformation and seismicity of Campi Flegrei caldera (Italy), during the 2000–2023 unrest, *Communications Earth & Environment*, 5, 742, <https://doi.org/10.1038/s43247-024-01865-y>, 2024.
- Bonferroni, C.: Teoria statistica delle classi e calcolo delle probabilità, *Pubblicazioni del Regio Istituto Superiore di Scienze Economiche e Commerciali di Firenze*, 8, 3–62, 1936 (in Italian).
- Buono, G., Maccaferri, F., Pappalardo, L., Tramelli, A., Caliro, S., Chiodini, S., Pinel, V., Rivalta, E., Spagnuolo, E., Trasatti, E., and Di Vito, M. A.: Weak Crust Owing Past Magmatic Intrusions Beneath Campi Flegrei Identified: The Engine for Bradyseismic Movements?, *AGU Advances*, 6, e2024AV001611, <https://doi.org/10.1029/2024AV001611>, 2025.
- Capuano, P., Russo, G., Civetta, L., Orsi, G., D’Antonio, M., and Moretti, R.: The active portion of the Campi Flegrei caldera structure imaged by 3-D inversion of gravity data, *Geochem. Geophys. Geosy.*, 14, 4681–4697, <https://doi.org/10.1002/ggge.20276>, 2013.
- Castaldo, R., Tizzani, P., and Solaro, G.: Inflating Source Imaging and Stress/Strain Field Analysis at Campi Flegrei Caldera: The 2009–2013 Unrest Episode, *Remote Sens.*, 13, 2298, <https://doi.org/10.3390/rs13122298>, 2021.
- Charlton, D., Kilburn, C., and Edwards, S.: Volcanic unrest scenarios and impact assessment at Campi Flegrei caldera, Southern Italy, *Journal of Applied Volcanology*, 9, 7, <https://doi.org/10.1186/s13617-020-00097-x>, 2020.
- Connor, C. B., Connor, L. J., Germa, A., Richardson, J. A., Bebbington, M., Gallant, E., and Saballos, J. A.: How to use kernel density estimation as a diagnostic and forecasting tool for distributed volcanic vents, *Statistics in Volcanology*, 4, 1–25, <https://doi.org/10.5038/2163-338X.4.3>, 2019.
- D’Auria, L., Massa, B., Cristiano, E., Del Gaudio, C., Giudicepietro, F., Ricciardi, G., and Ricco, C.: Retrieving the stress field within the Campi Flegrei caldera (Southern Italy) through an integrated geodetical and seismological approach, *Pure Appl. Geophys.*, 172, 3247–3263, <https://doi.org/10.1007/s00024-014-1004-7>, 2015.
- Del Gaudio, C., Aquino, I., Ricciardi, G. P., Ricco, C., and Scandone, R.: Unrest episodes at Campi Flegrei: A reconstruction of vertical ground movements during 1905–2009, *J. Volcanol. Geoth. Res.*, 195, 48–56, <https://doi.org/10.1016/j.jvolgeores.2010.05.014>, 2010.
- De Landro, G., Vanorio, T., Muzellec, T., Russo, G., Lomax, A., Virieux, J., and Zollo, A.: 3D structure and dynamics of Campi Flegrei enhance multi-hazard assessment, *Nat. Commun.*, 16, 4814, <https://doi.org/10.1038/s41467-025-59821-z>, 2025.
- Di Vito, M. A., Isaia, R., Orsi, G., Southon, J., de Vita, S., D’Antonio, M., Pappalardo, L., and Piochi, M.: Volcanism and deformation since 12,000 years at the Campi Flegrei caldera (Italy), *J. Volcanol. Geoth. Res.*, 91, 221–246, [https://doi.org/10.1016/S0377-0273\(99\)00037-2](https://doi.org/10.1016/S0377-0273(99)00037-2), 1999.
- Di Vito, M. A., Acocella, V., Aiello, G., Barra, D., Battaglia, M., Carandente, A., Del Gaudio, C., De Vita, S., Ricciardi, G. P., Ricco, C., Scandone, R., and Terrasi, F.: Magma transfer at Campi Flegrei caldera (Italy) before the 1538 AD eruption, *Scientific Reports*, 6, 32245, <https://doi.org/10.1038/srep32245>, 2016.
- Fernandez, G., Giaccio, B., Costa, A., Monaco, L., Nomade, S., Albert, P. G., Pereira, A., Flynn, M., Leicher, N., Lucchi, F., Petrosino, P., Palladino, D. M., Milia, A., Insinga, D. D., Wulf, S., Kearney, R., Veres, D., Jordanova, D., Putignano, M. L., Isaia, R., and Sottili, G.: New constraints on the Middle–Late Pleistocene Campi Flegrei explosive activity and Mediterranean tephrostratigraphy (~ 160 ka and 110–90 ka), *Quaternary Sci. Rev.*, 331, 108623, <https://doi.org/10.1016/j.quascirev.2024.108623>, 2024.
- Giaccio, B., Hajdas, I., Isaia, R., Deino, A., and Nomade, S.: High-precision  $^{14}\text{C}$  and  $^{40}\text{Ar}/^{39}\text{Ar}$  dating of the Campanian Ignimbrite (Y-5) reconciles the time-scales of climatic-cultural processes at 40 ka, *Scientific Reports*, 7, 45940, <https://doi.org/10.1038/srep45940>, 2017.

- Gibbons, J. D. and Chakraborti, S.: Non-parametric Statistical Inference, 4th edn., Marcel Dekker, New York, 645 pp., <https://doi.org/10.4324/9780203911563>, 2003.
- Gregg, P. M., de Silva, S. L., Grosfils, E. B., and Parmigiani, J. P.: Catastrophic caldera-forming eruptions: Thermomechanics and implications for eruption triggering and maximum caldera dimensions on Earth, *J. Volcanol. Geoth. Res.*, 241–242, 1–12, <https://doi.org/10.1016/j.jvolgeores.2012.06.009>, 2012.
- Isaia, R., Vitale, S., Marturano, A., Aiello, G., Barra, D., Ciarcia, S., Iannuzzi, E., and Tramparulo, F. D'A.: High-resolution geological investigations to reconstruct the long-term ground movements in the last 15 kyr at Campi Flegrei caldera (southern Italy), *J. Volcanol. Geoth. Res.*, 385, 143–158, <https://doi.org/10.1016/j.jvolgeores.2019.07.012>, 2019.
- Marzocchi, W., Taroni, M., and Selva, J.: Accounting for Epistemic Uncertainty in PSHA: Logic Tree and Ensemble Modeling, *B. Seismol. Soc. Am.*, 105, <https://doi.org/10.1785/0120140131>, 2015.
- Marzocchi, W., Selva, J., and Jordan, T. H.: A unified probabilistic framework for volcanic hazard and eruption forecasting, *Nat. Hazards Earth Syst. Sci.*, 21, 3509–3517, <https://doi.org/10.5194/nhess-21-3509-2021>, 2021.
- Meletti, C., Marzocchi, W., D'Amico, V., Lanzano, G., Luzi, L., Martinelli, F., Pace, B., Rovida, A., Taroni, M., Visini, F., Akinci, A., and Anzidei, M.: The new Italian seismic hazard model (MPS19), *Ann. Geophys.-Italy*, 64, SE112, <https://doi.org/10.4401/ag-8579>, 2021.
- Monaco, L., Palladino, D. M., Albert, P. G., Arienzo, I., Conticelli, S., Di Vito, M., Fabbriozzi, A., D'Antonio, M., Isaia, R., Manning, C. J., Nomade, S., Pereira, A., Petrosino, P., Sottili, G., Sulpizio, R., Zanchetta, G., and Giaccio, B.: Linking the Mediterranean MIS 5 tephra markers to Campi Flegrei (southern Italy) 109–92 ka explosive activity and refining the chronology of MIS 5c-d millennial-scale climate variability, *Global Planet. Change*, 211, 103785, <https://doi.org/10.1016/j.gloplacha.2022.103785>, 2022.
- Natale, J., Ferranti, L., Isaia, R., Marino, C., Sacchi, M., Spiess, V., Steinmann, L., and Vitale, S.: Integrated on-land-offshore stratigraphy of the Campi Flegrei caldera: New insights into the volcano-tectonic evolution in the last 15 kyr, *Basin Res.*, 34, 855–882, <https://doi.org/10.1111/bre.12643>, 2022.
- Natale, J., Vitale, S., Repola, L., Monti, L., and Isaia, R.: Geomorphic analysis of digital elevation model generated from vintage aerial photographs: A glance at the pre-urbanization morphology of the active Campi Flegrei caldera, *Geomorphology*, 460, 109267, <https://doi.org/10.1016/j.geomorph.2024.109267>, 2024.
- Natale, J., Cascella, E., and Vitale, S.: Tracking the growth and deformation of fissure phreatomagmatic eruptions: Insights from the ca. 3.9 ka Nisida eruption at Campi Flegrei caldera, southern Italy, *GSA Bulletin*, 2025, <https://doi.org/10.1130/B38367.1>, 2025.
- Orsi, G., Di Vito, M. A., and Isaia, R.: Volcanic hazard assessment at the restless Campi Flegrei caldera, *B. Volcanol.*, 66, 514–530, <https://doi.org/10.1007/s00445-003-0336-4>, 2004.
- Orsi, G., Di Vito, M. A., Selva, J., and Marzocchi, W.: Long-term forecasting of eruption style and size at Campi Flegrei caldera (Italy), *Earth Planet. Sc. Lett.*, 287, 265–276, <https://doi.org/10.1016/j.epsl.2009.08.013>, 2009.
- Pappalardo, L., Civetta, L., D'Antonio, M., Deino, A. L., Di Vito, M. A., Orsi, G., Caradente, A., De Vita, S., Isaia, R., and Piochi, M.: Chemical and Sr-isotopical evolution of the Phlegraean magmatic system before the Campanian Ignimbrite (37 ka) and the Neapolitan Yellow Tuff (12 ka) eruptions, *J. Volcanol. Geoth. Res.*, 91, 141–166, [https://doi.org/10.1016/S0377-0273\(99\)00033-5](https://doi.org/10.1016/S0377-0273(99)00033-5), 1999.
- Rivalta, E., Corbi, F., Passarelli, L., Acocella, V., Davis, T., and Di Vito, M. A.: Stress inversions to forecast magma pathways and eruptive vent location, *Science Advances*, 5, eaau9784, <https://doi.org/10.1126/sciadv.aau9784>, 2019.
- Scarpati, C., Perrotta, A., Lepore, S., and Calvert, A.: Eruptive history of Neapolitan volcanoes: Constraints from <sup>40</sup>Ar/<sup>39</sup>Ar dating, *Geol. Mag.*, 150, 412–425, <https://doi.org/10.1017/S0016756812000854>, 2013.
- Selva, J., Orsi, G., Di Vito, M. A., Marzocchi, W., and Sandri, L.: Probability hazard map for future vent opening at the Campi Flegrei caldera, Italy, *B. Volcanol.*, 74, 497–510, <https://doi.org/10.1007/s00445-011-0528-2>, 2012.
- Selva, J., Costa, A., De Natale, G., Di Vito, M. A., Isaia, R., and Macedonio, G.: Sensitivity test and ensemble hazard assessment for tephra fallout at Campi Flegrei, Italy, *J. Volcanol. Geoth. Res.*, 351, 1–28, <https://doi.org/10.1016/j.jvolgeores.2017.11.024>, 2018.
- SSHAC (Senior Seismic Hazard Analysis Committee): Recommendations for Probabilistic Seismic Hazard Analysis: Guidance on Uncertainty and Use of Experts, U.S. Nuclear Regulatory Commission, U.S. Dept. of Energy, Electric Power Research Institute, NUREG/CR-6372, UCRL-ID-122160, Vols. 1/2, <https://doi.org/10.2172/479072>, 1997.
- Sparice, D., Pelullo, C., de Vita, S., Arienzo, I., Petrosino, P., Mormone, A., Di Vincenzo, G., Marfè, B., Cariddi, B., De Lucia, M., Vertech, E., D'Oriano, C., Del Carlo, P., Di Roberto, A., Giaccio, B., Zanchetta, G., and Di Vito, M. A.: The pre-Campi Flegrei caldera (> 40 ka) explosive volcanic record in the Neapolitan Volcanic Area: New insights from a scientific drilling north of Naples, *J. Volcanol. Geoth. Res.*, 455, 108209, <https://doi.org/10.1016/j.jvolgeores.2024.108209>, 2024.
- Tarquini, S., Isola, I., Favalli, M., Battistini, A., and Dotta, G.: TINI-TALY, a digital elevation model of Italy with a 10 meters cell size, Version 1.1, Istituto Nazionale di Geofisica e Vulcanologia (INGV) [data set], <https://doi.org/10.13127/tinitaly/1.1>, 2023.
- Vitale, S. and Natale, J.: Combined volcano-tectonic processes for the drowning of the Roman western coastal settlements at Campi Flegrei (southern Italy), *Earth Planets Space*, 75, 38, <https://doi.org/10.1186/s40623-023-01795-7>, 2023.